ＩＳＳＮ１３４６－７８３２

独立行政法人港湾空港技術研究所

港湾空港技術研究所報告

REPORT OF THE PORT AND AIRPORT RESEARCH INSTITUTE

VOL.49　NO.2　June 2010

NAGASE, YOKOSUKA, JAPAN

INDEPENDENT ADMINISTRATIVE INSTITUTION,
PORT AND AIRPORT RESEARCH INSTITUTE

港湾空港技術研究所報告（REPORT OF PARI）

第 49 巻　第 2 号（Vol. 49，No. 2），　2010年6月（June 2010）

目　　次（CONTENTS）

REPORT OF THE PORT AND
AIRPORT RESEARCH INSTITUTE
Vol.49, No.2 (June 2010)

One-Dimensional Model for Undertow and Longshore Current Velocities in the Surf Zone

Yoshiaki KURIYAMA*

Synopsis

A one-dimensional model for undertow and longshore current velocities assuming a triangular velocity distribution in a surface roller was developed. This model as well as a model with the assumption of a uniform velocity distribution in a roller was compared with field data obtained on barred beaches at Hasaki in Japan and at Duck in the USA. The comparisons showed that the present model predicted the velocity fields at the two sites reasonably well, and the prediction accuracy of the present model is slightly better than that of the other model. However, the present model underpredicted the undertow velocities on the trough regions, and overestimated the longshore current velocities near the shorelines.

Key Words: numerical model, undertow, longshore current, surface roller, surf zone

* Head, Coastal Sediments and Processes Group, Marine Environment and Engineering Department
Nagase 3-1-1, Yokosuka, Kanagawa 239-0826, Japan
Phone：+81-46-844-5045 Fax：+81-46-841-9812 e-mail: kuriyama@pari.go.jp

港湾空港技術研究所報告
第 49 巻第 2 号(2010. 6)

戻り流れ速度・沿岸流速に関する数値モデル

栗山　善昭*

要　　旨

戻り流れ速度と沿岸流速を，精度良く，かつ，計算負荷を少なく推定するために，砕波帯内で発達する surface roller の鉛直分布として三角形分布（上端で波速，下端でゼロ）を仮定する 1 次元のパラメトリックモデルを開発した．本モデルの現地適用性を，surface roller の鉛直分布として一定値（波速）を仮定している既存のモデルの適用性とともに，茨城県波崎海岸およびアメリカ東海岸 Duck で取得された戻り流れ・沿岸流速データで検証した．その結果，本モデルはトラフ領域における戻り流れ速度を過小評価するとともに，汀線近傍の沿岸流速を過大評価しているものの，全体的に，計算値は実測値と良い一致を示した．本モデルと既存のモデルの推定精度を比較すると，本モデルの精度の方が既存のモデルの精度に比べて若干高かった．

キーワード：数値モデル，戻り流れ，沿岸流，砕波帯

* 海洋・水工部　沿岸環境領域　沿岸土砂管理研究チーム
〒239-0826　横須賀市長瀬3-1-1　独立行政法人　港湾空港技術研究所
電話：046-844-5045　Fax：046-841-9812　　e-mail: kuriyama@pari.go.jp

CONTENTS

1. Introduction

A lot of sandy beaches suffer from beach erosion problems, and plenty of ports and harbors experience sedimentation problems. Those problems are caused by sediments transported by nearshore currents in the nearshore zone, consisting of cross-shore and longshore currents. Hence, in order to find effective countermeasures, predicting cross-shore and longshore current velocities is essential.

Cross-shore and longshore current velocities in the nearshore zone are strongly influenced by wave breaking. The laboratory experiments for cross-shore velocity in and outside the surf zone by Nadaoka and Kondoh (1982) showed that the shoreward mass flux above the wave trough level in the surf zone is several times larger than that outside the surf zone owing to wave breaking. In order to express the additional mass, momentum and energy fluxes due to wave breaking, Svendsen (1984) proposed the concept of a surface roller, which is located above the wave trough level and contains water transported shoreward, and developed a model including the surface roller for the velocity of the time-averaged cross-shore current, referred to as undertow, in and outside the surf zone.

Undertow models including the surface roller contribution were also developed by Stive and Wind (1986), Okayasu et al. (1986), de Vriend and Stive (1987), Deigaard et al. (1991), Smith et al. (1992), Cox and Kobayashi (1998), Kuriyama and Nakatsukasa (2000) and others, while Dally and Dean (1984), Haines and Sallenger, Jr. (1994) and Masselink and Black (1995) formulated undertow models without the surface roller. The surface roller models were further developed by Nairn et al. (1990), Okayasu et al. (1990), Stive and de Vriend (1994), Dally and Brown (1995) and Renier and Battjes (1997), who modeled the evolution of a surface roller including consideration of energy balance for waves and rollers.

As for the longshore current, Longuet-Higgins (1970a, b), Thornton and Guza (1986) and Larson and Kraus (1991) developed models for the longshore current velocity in and outside the surf zone, which do not include the surface roller, and showed that the models agreed reasonably well with laboratory or field data on planar beaches. However, model predictions without the surface roller have some discrepancies with the measurements on barred beaches. Those models were not able to reproduce relatively large velocities in trough regions (Church and Thornton, 1993; Kuriyama and Ozaki, 1993; Smith et al., 1993).

In order to overcome the problem, Church and Thornton (1993) and Smith et al. (1993) considered the turbulence due to wave breaking for longshore current velocity prediction. Kuriyama (1994) incorporated the surface roller model by Svendsen (1984) into a longshore current model and showed that the incorporation of the surface roller resulted in the shoreward shifts of the maximum longshore current velocities over bar crests and reproduced the large velocities in trough regions, while Osciecki and Dally (1996) also included the surface roller evolution model developed by Dally and Brown (1995) and showed that the location of the peak longshore current velocity predicted with the surface roller shifted shoreward from that without the roller on a planar beach. Although Lippmann et al. (1995) and Renier and Battjes (1997) concluded that including the effect of a surface roller alone cannot reproduce large velocities in trough regions, Kuriyama and Nakatsukasa (2000) and Ruessink et al. (2001) showed that the inclusion of the surface roller increases the accuracy of the longshore current prediction in bar-trough regions.

Because the surface roller evolution has strong influence on the undertow and longshore current velocities in the surf zone as mentioned above, the model prediction accuracies for the undertow and longshore current velocities should be tested with both of the velocities measured at the same locations and over the same periods under a wide range of conditions. However, such verifications were rarely conducted, in particular with field data, except in Kuriyama and Nakatsukasa (2000) and Grasmeijer and Ruessink (2003).

Grasmeijer and Ruessink (2003) investigated the accuracies of probabilistic and parametric models for the estimations of undertow and longshore current velocities with field data obtained on the Egmond coast in the Netherlands and at Duck in the USA. The probabilistic models are based on the transformations of individual waves or 10 to 12 representative waves, whereas the parametric models are based on that of a representative wave such as a wave with the root-mean-square wave height, the peak wave period and the principal wave direction (van Rijn and Wijnberg, 1996; Grasmeijer and Ruessink, 2003). Most of the undertow and longshore current velocities estimated by both models using the surface roller contribution in Svendsen (1984) and the roller evolution model in Stive and de Vriend (1994) agreed

well with the measured ones although the undertow velocities on the bar crests were underestimated by both the models.

Kuriyama and Nakatsukasa (2000) proposed a probabilistic model for estimating undertow and longshore current velocities, and showed that the model estimated undertow and longshore current velocities on barred beaches reasonably well. However, the model assumed that the surface roller area is proportional to the square of the wave height in a region where the wave is breaking as in Svendsen (1984) and hence has the drawback that the surface roller area suddenly drops to zero when the breaking wave recovers.

Furthermore, Kuriyama and Nakatsukasa's model, which adopts the wave-by-wave approach, is time-consuming although predictions of long-term beach profile changes require time-effective models such as parametric ones for predicting waves and currents.

The objectives of this paper are to develop a one-dimensional parametric model for undertow and longshore current velocities by modifying the probabilistic model of Kuriyama and Nakatsukasa (2000), which was shown to predict undertow and longshore current velocities on barred beaches reasonably well, and to verify the prediction accuracies for both the undertow and longshore current velocities with field data obtained on barred beaches at Hasaki in Japan and at Duck in the USA.

In Section 2, the numerical model is described. Using field data explained in Section 3, the model is calibrated in Section 4. The validity of the model is examined and discussed in Sections 5 and 6 by comparing undertow and longshore current velocities predicted and measured in the field and using the qualifications of error ranges defined by van Rijn et al. (2003). The qualifications are based on relative mean absolute error ε_{rms}, of which the definition is shown in 4.3, and predictions with ε_{rms}<0.01, 0.1-0.3, 0.3-0.5, 0.5-0.7 and >0.7 are qualified as Excellent, Good, Reasonable, Poor and Bad. The conclusions are shown in Section 7.

2. Numerical model

The numerical model is one-dimensional and parametric, and consists of three sub-models for wave transformation, for the undertow velocity and for the longshore current velocity.

2.1 Wave transformation

Although Kuriyama and Nakatsukasa's model (2000) calculates the transformation of individual waves, the present model estimates the cross-shore variation of the root-mean-square wave height H_{rms}, which is used in the estimations of the undertow and longshore current velocities, assuming a Rayleigh distribution as the wave height probability density function over an entire computational domain as in Thornton and Guza (1983). The energy of waves with heights larger than the breaking wave height is dissipated.

The breaking wave height is estimated with the formula (Eq. (1)) proposed by Seyama and Kimura (1988), who improved Goda's criterion (1970) using their experimental data.

$$\frac{H_b}{h_b}=C_{br}\left[0.16\frac{L_0}{h_b}\left\{1-\exp\left[-0.8\pi\frac{h_b}{L_0}\left(1+15\tan^{4/3}\beta\right)\right]\right\}-0.96\tan\beta+0.2\right] \tag{1}$$

where H_b is the breaking wave height, h_b is the breaking water depth, C_{br} is a nondimensional coefficient, L_0 is the offshore wavelength and $\tan\beta$ is the beach slope. The nondimensional coefficient C_{br} was introduced by Kuriyama (1996) to fit Seyama and Kimura's formula to field data. The beach slope is defined to be positive for the water depth increasing seaward and estimated as the average slope in a 30-meter-long region of which the definition point is located at the center.

The wave energy dissipation is estimated using the periodic bore model proposed by Thornton and Guza (1983).

$$\frac{\partial E_w C_g\cos\theta}{\partial x}=\int_{H_b}^{\infty}P(H)B(H)dH$$
$$B(H)=\frac{1}{4}\rho g\frac{1}{T}\frac{(B_w H)^3}{h} \tag{2}$$

where E_w is the wave energy, C_g is the group velocity, θ is the wave direction defined relative to the shoreward direction, x is the seaward distance, $P(H)$ is the probability density of the wave height, ρ is the seawater density, T is the wave period, H is the wave height, and h is the water depth including the wave setup and setdown. A nondiemnsional parameter B_w obtained by Kuriyama and Ozaki (1996) using Seyama and Kimura's experimental data (1988) is expressed as

$$B_W=C_B\left\{1.6-0.12\ln(H_0/L_0)+0.28\ln(\tan\beta)\right\} \tag{3}$$

where H_0 is the offshore wave height and C_B is a

nondimensional coefficient.

The peak wave period is used as the wave period in the calculation as in Grasmeijer and Ruessink (2003). The significant wave height is estimated as $H_{1/3} = 1.416\, H_{rms}$.

2.2 Undertow velocity

The vertically averaged undertow velocity U is estimated from Eq. (4) as in Svendsen (1984).

$$U = \frac{Q_W + Q_r}{d_{tr}} \tag{4}$$

where Q_w and Q_r are the mass fluxes due to waves and surface rollers, respectively. The value of d_{tr} represents the distance between the wave trough level and the bottom, and is assumed to be $d_{tr} = h - H_{rms}/2$.

Equation (5), which was also proposed by Svendsen (1984), is used for the estimation of Q_w.

$$Q_W = \frac{C}{h}\zeta_{rms}^2 \tag{5}$$

where C is the celerity and ζ_{rms} is the standard deviation of water surface elevation of a wave, which is obtained from Eq. (6) with a parameter Π for wave nonlinearity proposed by Goda (1983).

$$\zeta_{rms} = \frac{1}{2\sqrt{2}} H_{rms}, \qquad \Pi < 0.15$$

$$\zeta_{rms} = \frac{1}{1.668 \log_{10} \Pi_{rms} + 4.204} H_{rms}, \qquad 0.15 \le \Pi < 3$$

$$\zeta_{rms} = \frac{1}{5} H_{rms}, \qquad \Pi \ge 3 \tag{6}$$

$$\text{with} \quad \Pi = \frac{H_{rms}}{L} \tanh^3 \frac{2\pi h}{L} \tag{7}$$

where L is the wavelength.

The value of Q_r is estimated under the assumption that the vertical distribution of the cross-shore velocity in a surface roller is triangular with the celerity C at the top of the roller and zero at the bottom (**Figure 1**) as in Kuriyama and Nakatsukasa (2000).

$$Q_r = \frac{A_r C}{2L} \tag{8}$$

where A_r is the area of a surface roller.

Although Kuriyama and Nakatsukasa (2000) assumed that a surface roller exists only in the wave breaking zone and A_r is proportional to H^2, the assumption is unnatural because A_r abruptly drops to zero in the model when a wave propagates from the breaking zone to the reforming zone. Hence, to

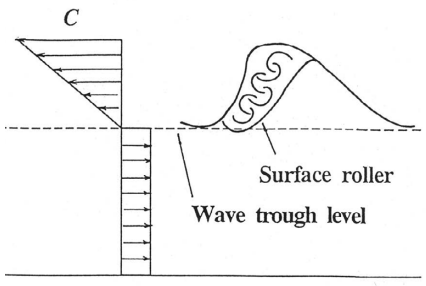

Figure 1 Assumed vertical distribution of time-averaged cross-shore velocity.

reproduce the smooth development and decay of a roller, A_r is estimated on the basis of the energy balance as in de Vriend and Stive (1987), and Dally and Brown (1995). However, because preliminary calculations with the surface roller energy dissipation term proposed by de Vriend and Stive (1987) sometimes underestimated the roller energy dissipation in a very shallow area, which resulted in an extraordinarily large velocity, A_r/h^2 was inserted into the surface roller energy dissipation term in order to suppress the unusual increase in undertow velocity near the shoreline. The energy balance in a surface roller is expressed as

$$\frac{\partial (E_W C_g \cos\theta)}{\partial x} + \frac{\partial (F_r \cos\theta)}{\partial x} = D_r, \qquad F_r = \frac{1}{8}\rho C^3 \frac{A_r}{L}$$

$$D_r = B_r \frac{g F_r}{C^2} \frac{A_r}{h^2} \tag{9}$$

where F_r is the surface roller energy flux, D_r is the energy dissipation rate of the surface roller and B_r is a nondimensional coefficient.

2.3 Longshore current velocity

The vertically averaged longshore current velocity V is estimated from Eq. (10), which represents the radiation stress R_x, the wind stress W_x, the momentum flux due to a surface roller M_x, the lateral mixing term L_x and the momentum balance among the friction term F_x.

$$R_x - W_x + M_x - L_x + F_x = 0 \tag{10}$$

The radiation stress term R_x is estimated using the small amplitude theory.

$$R_x = \frac{1}{\rho h}\left(\frac{\partial S_{yx}}{\partial x}\right), \qquad S_{yx} = \rho g \frac{C_g}{C}\frac{1}{8} H_{rms}^2 \cos\theta \sin\theta \tag{11}$$

The wind stress term W_x is assumed to be

$$W_x = \frac{1}{\rho h} C_d \rho_a W_v^2 \sin\alpha_w \tag{12}$$

where C_d is a nondimensional coefficient, ρ_a is the air density, W_v is the wind velocity and α_w is the wind direction. The value of C_d was assumed to be 0.0022 as in Kuriyama et al. (2008).

The momentum flux due to a surface roller M_x is expressed as

$$M_x = \frac{1}{\rho h}\left(\frac{\partial M_r}{\partial x}\right), \quad M_r = -\frac{1}{3}\rho_w C^2 \frac{A_r}{L}\cos\theta\sin\theta \tag{13}$$

The lateral mixing term L_x is assumed as in Ruessink et al. (2001) with a dimensional coefficient ν.

$$L_x = \frac{\partial}{\partial x}\left(\varepsilon\frac{\partial V}{\partial x}\right), \quad \varepsilon = \nu h \tag{14}$$

The friction term F_x proposed by Nishimura (1988) is used in the model.

$$F_x = \frac{C_f}{h}\left(W + \frac{w_b^2}{W}\sin^2\theta\right)V$$
$$W = \frac{\sqrt{V^2 + w_b^2 + 2Vw_b\sin\theta} + \sqrt{V^2 + w_b^2 - 2Vw_b\sin\theta}}{2}$$
$$w_b = \frac{2v_m}{\pi}, \quad v_m = \frac{\pi H_{rms}}{T\sinh\left(\frac{2\pi h}{L}\right)} \tag{15}$$

where C_f is a nondimensional coefficient and v_m is the amplitude of the orbital velocity at the bottom.

Kuriyama and Nakatsukasa (2000) showed that the longshore current model with C_f = 0.005 well predicted the longshore current velocity on and around a longshore bar at Hasaki. However, Garcez-Fariaet et al. (1998) showed, on the basis of field data, that the friction coefficient is not constant in the cross-shore direction and even at Hasaki, the longshore current velocity outside the surf zone was overestimated using the model with C_f = 0.005. Hence, as in Garcez-Faria et al. (1998) and Ruessink et al. (2001) the friction coefficient is assumed to be a function of the water depth as expressed by Eq. (16) with the apparent bed roughness k_a.

$$C_f = 0.015\left(\frac{k_a}{h}\right)^{1/3} \tag{16}$$

3. Field data

Two field data sets were compared with the model. One was obtained at the Hasaki coast in eastern Japan facing the Pacific Ocean (Kuriyama, 1998) and the other was obtained on a barrier island facing the Atlantic Ocean near Duck in the USA during the Duck94 field measurement (Elgar et al., 1997; Feddersen et al., 1998; Gallagher et al., 1998).

3.1 Hasaki data

The undertow and longshore current velocity data were obtained along a 427-meter-long pier of the Hazaki Oceanographical Research Station (HORS) during a period from January 30 to February 3, 1997. Cross-shore and longshore current velocities were measured with four electro-magnetic current meters installed on and around a longshore bar at a sampling frequency of 5 Hz for 30 minutes every 2 hours and water surface elevations were measured with five ultrasonic wave gages (**Figure 2**). Wind angle and velocity were measured at the tip of the pier for 10 minutes every hour. Offshore wave heights and periods were measured with an ultrasonic wave gage for 20 minutes every 2 hours about 5 km north of HORS at a water depth of about 24 m.

The beach profiles along the pier were measured at 5 m intervals every day, except for weekends and holidays, with a 5 kg lead from the pier, and with a level and a staff shoreward

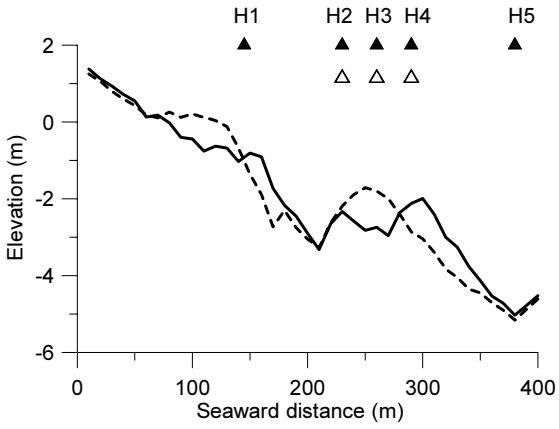

Figure 2 Locations of current meters (open triangles) and wave gages (solid triangles), and beach profiles at Hasaki. The profiles on January 30 and February 3 in 1997 are represented by the broken and solid lines, respectively. The numbers with the letter “H” above the solid triangles show the location numbers.

of the pier. The longshore bar migrated seaward during the measurement (**Figure 2**) owing to high waves caused by a developed depression. The seaward bar migration damaged the supporting systems of the instruments, which caused some missing data.

3.2 Duck data

The undertow and longshore current velocities and the water surface elevations were measured with 10 electro-magnetic current meters and 14 pressure gages (**Figure 3**) at a frequency of 2 Hz for 1024 s every 3 hours about 400 m north of the U.S. Army Corps of Engineers Field Research Facility (FRF). The data obtained during a period from September 21 to 23, 1994, were compared with the model as in Grasmijer and Ruessink (2003). At a water depth of about 8 m, the wave heights, periods and directions were measured by a two-dimensional array of 15 pressure sensors at a sampling frequency of 2 Hz for 8192 s every 3 hours. Wind velocity and direction were measured at the seaward tip of a pier of FRF, about 500 m from the shore.

The bathymetry at the measurement site was measured with the Coastal Research Amphibious Buggy (CRAB) several times during the two-month Duck94 experiment. Although high waves attacked the study site on September 22, the longshore bar was rather stable and the beach profile change during the measurement period was small (**Figure 3**).

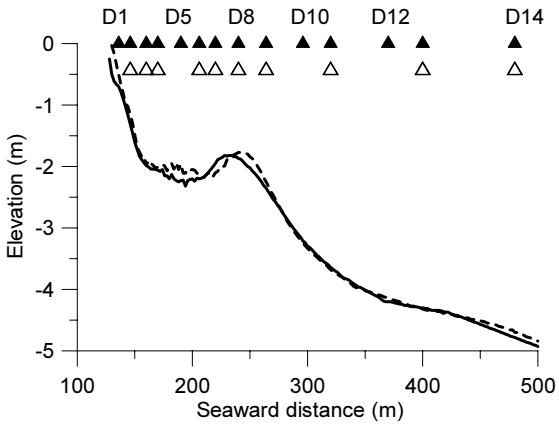

Figure 3 Locations of current meters (open triangles) and wave gages (solid triangles), and beach profiles at Duck. The profiles on September 21 and 24 in 1994 are represented by the broken and solid lines, respectively. The numbers with the letter "D" above the solid triangles show the location numbers.

4. Calibration

4.1 Model setup

(1) Hasaki

The temporal interval for the calculation was set to 2 hours, and the space grid interval was set to 2 m. The seaward boundary was located where the seaward distance was 920 m and the water depth was about 9 m. The input significant wave heights and periods were estimated from those measured offshore. The input mean wave angles were estimated from those measured at H4 using Snell's law and the input water levels were set to be equal to those at H5 (**Figure 2**) (Kuriyama, 1998). The ranges of the significant wave height and period and the mean incident wave angle at the boundary were from 1.7 to 2.6 m, from 9.7 to 12.2 s and from 4.8 to 26.7 degrees, respectively (**Figure 4**).

The beach profiles shoreward of the tip of the pier, where the seaward distance is 385 m, were linearly interpolated at intervals of 2 hours with the profiles measured daily. In a region where the seaward distance was 445 m to 600 m, the profile surveyed on January 16, 1997 was used (Kuriyama, 1998), and the beach profiles between the tip of the pier and the cross-shore location of 445 m were linearly interpolated with the elevations at the seaward and shoreward edges of the region as in Kuriyama et al. (2008). Seaward of the

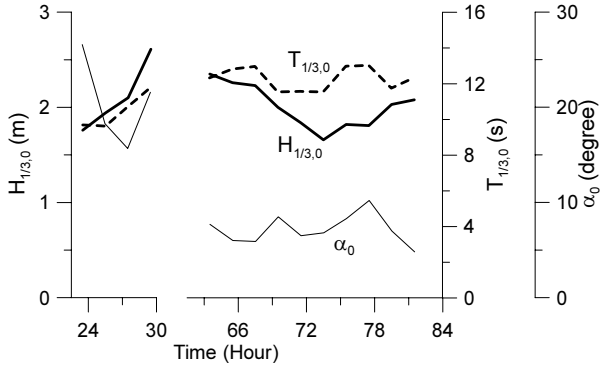

Figure 4 Time series of the significant wave height $H_{1/3,0}$ and period $T_{1/3,0}$ and the mean incident wave angle α_0 at the seaward boundary at Hasaki. The wave heights were estimated from the offshore wave heights taking into consideration wave shoaling and refraction. The wave periods were the values measured at H5. The wave angles were estimated using Snell's law and the wave angles measured at H2. Time = 0 corresponds to January 30, 1997, 00:00 hrs.

cross-shore location of 600 m, the mean profile obtained on the basis of the yearly bathymetry surveys around HORS (Kuriyama et al., 2008) was used.

(2) Duck

The calculation interval was 3 hours. The grid size was 2 m, and the seaward boundary was set at a distance of 884 m, where the water depth was about 8 m and the offshore wave data were collected. Although the significant wave height was low, 0.7 m, at the start of the measurement, it abruptly increased on the second day, reached 2.6 m and gradually decayed (**Figure 5**). The peak wave period varied between 3.7 to 9.9 s and the mean wave angle ranged from –30.0 to 20.6 degrees. The beach profiles were linearly interpolated with the profiles surveyed on September 16, 21 and 24.

4.2 Wave height

In order to reduce errors in the velocity predictions caused by the errors in wave height predictions, the parameters C_{br} and C_B in Eqs. (1) and (3) were determined in each case so that the error between the measured and predicted significant wave heights in each case was minimum. The numbers of the calculation cases are 14 at Hasaki and 16 at Duck.

The value of C_{br} ranged from 0.75 to 1.65, and C_B from 0.65 to 9.40. The error in the prediction of the significant wave height at each case ranged from 0.11 to 0.19 m at Hasaki and from 0.02 to 0.14 m at Duck.

4.3 Undertow and longshore current velocities

There are three free parameters in the undertow and longshore current sub-models, which are B_r in Eq. (9), ν in Eq. (14) and k_a in Eq. (16). These parameters were determined so that the mean value of the relative mean absolute errors in the undertow and longshore current velocities at Hasaki and Duck was minimum.

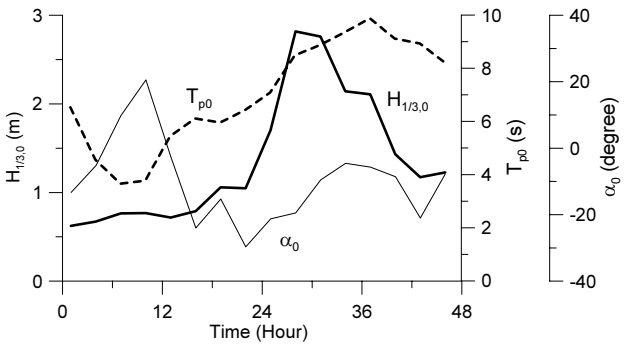

Figure 5 Time series of the significant wave height $H_{1/3,0}$, the peak wave period T_{p0} and the mean incident wave angle α_0 at the seaward boundary at Duck. Time = 0 corresponds to September 21, 1994, 01:00 EST.

The relative mean absolute errors ε_{rma} were defined as in van Rijn et al. (2003).

$$\varepsilon_{rma} = \frac{\sum_t \left(\left| X_{pred} - X_{meas} \right| - X_{error} \right)}{\sum_t \left| X_{meas} \right|} \tag{17}$$

where X_{meas} and X_{pred} are the measured and predicted velocities, respectively. The value of X_{error} is the measurement error, which was assumed to be 0.05 m/s as in van Rijn et al. (2003).

Because the undertow and longshore current velocities were measured at single heights at most of the measurement locations, the values predicted at the measurement heights are more suitable for the comparisons between the measured and predicted velocities than the vertically averaged ones. However, although the vertical distribution of longshore current velocity is relatively simple and easy to predict, that of undertow velocity is complex and no formula for predicting the vertical distribution of undertow velocity is fully verified with field data. Hence, in this study, the longshore current velocities at measurement points were predicted and compared with the measure values, but for undertow velocity, the vertically averaged values were used for the comparisons.

The vertical distribution of longshore current velocity V_z was estimated as

$$V_z = \frac{V_*}{\kappa} \ln\left(\frac{z}{z_a}\right) \tag{18}$$

where V_* is the shear velocity, κ is the von Karman constant (= 0.4), z is the height from the bottom and z_a is the apparent roughness height, which was assumed to be $k_a/30$ as in Garcez-Faria et al. (1998).

The mean value of ε_{rma} for the entire calibration $\overline{\varepsilon_{rma,all}}$ was obtained from four mean values of ε_{rma} for the undertow and longshore current velocities at Hasaki and Duck, and it is expressed by

$$\overline{\varepsilon_{rma,all}} = (\overline{\varepsilon_{rma,U,H}} + \overline{\varepsilon_{rma,L,H}} + \overline{\varepsilon_{rma,U,D}} + \overline{\varepsilon_{rma,L,D}}) / 4 \tag{19}$$

where $\overline{\varepsilon_{rma}}$ denotes the mean value of ε_{rma}, the subscripts U and L denote the values for the undertow and longshore current velocities, respectively, and the subscripts H and D denote the values at Hasaki and Duck, respectively.

The values of $\overline{\varepsilon_{rma}}$ were computed using the combinations of B_r ranging from 0.016 to 1.6, ν from 0.5 to 5.0 m^2/s and k_a from 0.02 to 0.5 m. The obtained minimum value of $\overline{\varepsilon_{rma}}$ is 0.369 and the best fit parameters are B_r = 0.096, ν = 0.5 m^2/s and k_a = 0.10 m.

5. Model comparisons with measurements

5.1 Hasaki

The relative mean absolute errors in the undertow and longshore current velocities defined by Eq. (17) at each measurement location at Hasaki are shown in **Figure 6**, which also shows the relative errors for another parametric model assuming a uniform velocity distribution in a surface roller as in Svendsen (1984) and employing the roller energy dissipation model proposed by Stive and de Vriend (1994). The mass flux due to rollers and the roller energy dissipation are expressed as

$$Q_r' = A_r' C / L \tag{20}$$

$$\frac{\partial (E_w C_g)}{\partial x} + \frac{\partial (2E_r' C)}{\partial x} = D_r', \quad E_r' = \frac{1}{2}\rho C^2 \frac{A_r'}{L}, \quad D_r' = B_r' \frac{2gE_r'}{C} \tag{21}$$

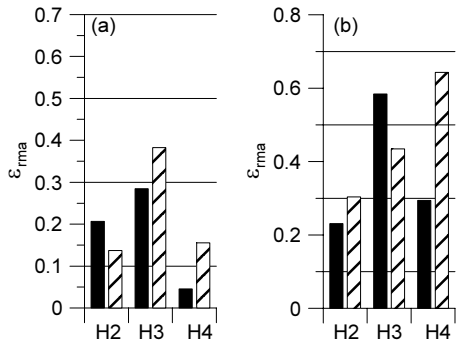

Figure 6 Model error statistics for the undertow (a) and longshore current (b) velocities at Hasaki. The solid and hatched columns show the values for the present parametric model and the previous parametric model, respectively.

In Eqs. (20) and (21), the primes represent the values under the assumption of a uniform distribution in a roller. The calculations were done with B_r' = sin(0.05), ν' =0.5 m^2/s and k_a' = 0.0125 m as in Ruessink et al. (2001). Hereafter, the model based on Eqs. (20) and (21) will be called the previous parametric model.

All of the errors of the undertow and longshore current velocities predicted by the present parametric model are lower than 0.3, the upper limit for good prediction (van Rijn et al., 2003), except for the error of longshore current velocity at H3.

The errors for the present parametric model are comparable to those for the previous parametric model in both of the undertow and longshore current velocities (**Figure 6**). However, the comparison between the velocities predicted by the present and previous parametric models shows that the undertow velocities predicted by the present parametric model are mostly larger than those by the previous parametric model (**Figure 7**), while there is no such tendency in the longshore current velocity.

5.2 Duck

In the undertow velocity prediction using the present parametric model, two errors out of ten are lower than 0.1, upper limit of excellent prediction and six errors range from 0.1 to 0.3 (**Figure 8**). At D9, where the previous parametric model predicted the undertow velocities reasonably well, the error of the present parametric model is higher than 0.7. The errors at D6 for the present and previous parametric models are higher than 0.5. Although the previous parametric model also had similar prediction accuracy as the present parametric model (**Figure 8**), the previous one tended to underestimate the undertow velocities in the surf zone (**Figure 9**).

Compared with the undertow velocity prediction, the longshore current velocity prediction using the present parametric model as well as that using the previous parametric model was relatively poor, in particular near the shoreline, at D2. In the present model's prediction, one error is lower than 0.3 and seven errors range from 0.3 to 0.5.

6. Discussion

The best-fit ν (0.5 m^2/s) in this study is equal to the value used in Ruessink et al. (2001). The value of k_a (0.10 m) is four to eight times the range (0.0125 to 0.022 m) in Ruessink et al.

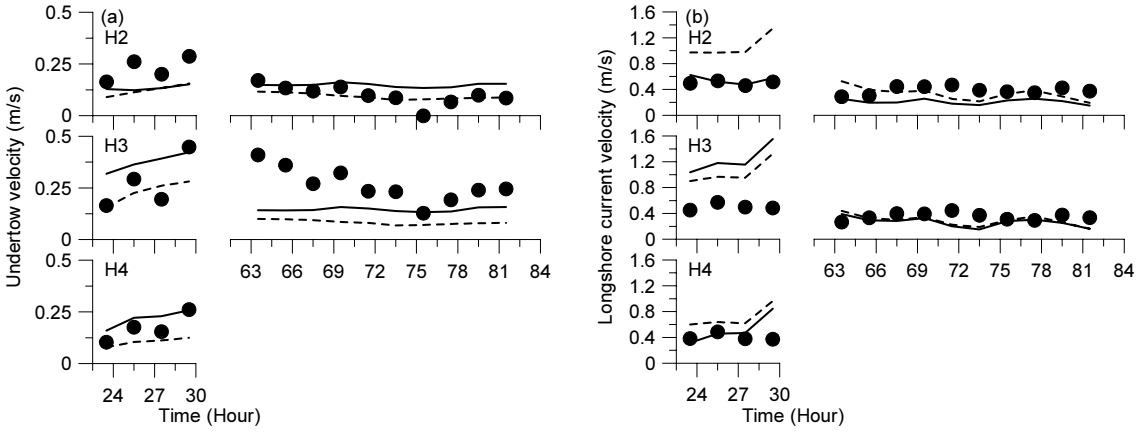

Figure 7 Time series of the undertow (a) and longshore current (b) velocities at Hasaki. The solid circles show the measured values. The thick solid and broken lines show the values predicted by the present previous parametric models, respectively. The predicted values are vertically averaged ones for undertow velocity (a) and those at the measurement points for longshore current velocity (b).

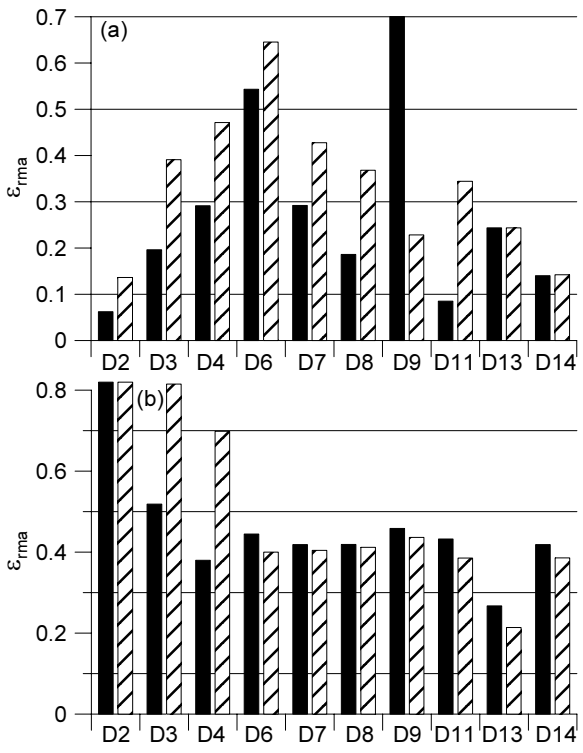

Figure 8 Model error statistics for the undertow (a) and longshore current (b) velocities at Duck. Although ε_{rma} in the longshore current velocity at D2 were 1.69 and 1.73 for the present and previous parametric models, respectively, those values were shown to be 0.82, which is slightly larger than the maximum value on the vertical scale in the figure. See **Figure 6** for an explanation of graphical symbols.

(2001), but well within the range (0.01 to 2.1 m) obtained by Garcez-Faria et al. (1998) on the basis of the vertical variation of longshore current velocity at Duck.

The best-fit B_r in Eq. (9) is 0.096, while Ruessink et al. (2001) used sin(0.05) for B_r' in Eq. (21). Because $F_r = (3/4)E_rC$, B_r is equivalent to $(8/3)/(A_r/h^2)B_r$'. Considering that A_r/h^2 was about 4 in the surf zone in this study, B_r is roughly equivalent to $2/3B_r$'. When the value used by Ruessink et al. (2001), sin(0.05), was substituted into B_r', the best-fit B_r (0.096) in this study was about three times $2/3B_r$'(0.033). The difference may be caused by the difference in the vertical velocity distribution in a surface roller.

The undertow velocity prediction with the present parametric model was poor at D9 at Duck as mentioned before. However, the measured velocities at D9 were lower than those at the neighboring measurement locations, D8 and D11, at $t > 25$ hours, when the wave height at the seaward boundary was large, as shown in **Figures 9 and 10**, and hence some measurement problem at D9 may have caused the poor prediction.

The poor prediction for the undertow velocity at D6 at Duck may also have been caused by a measurement problem. The undertow velocities at D6 were larger than those at the neighboring location, D4 and D7, in particular when the wave height at the seaward boundary was small (**Figures 9 and 11**).

Although the undertow velocity predictions by the present and pervious parametric models were mostly good or reasonable near the bar crests at the two sites, the previous

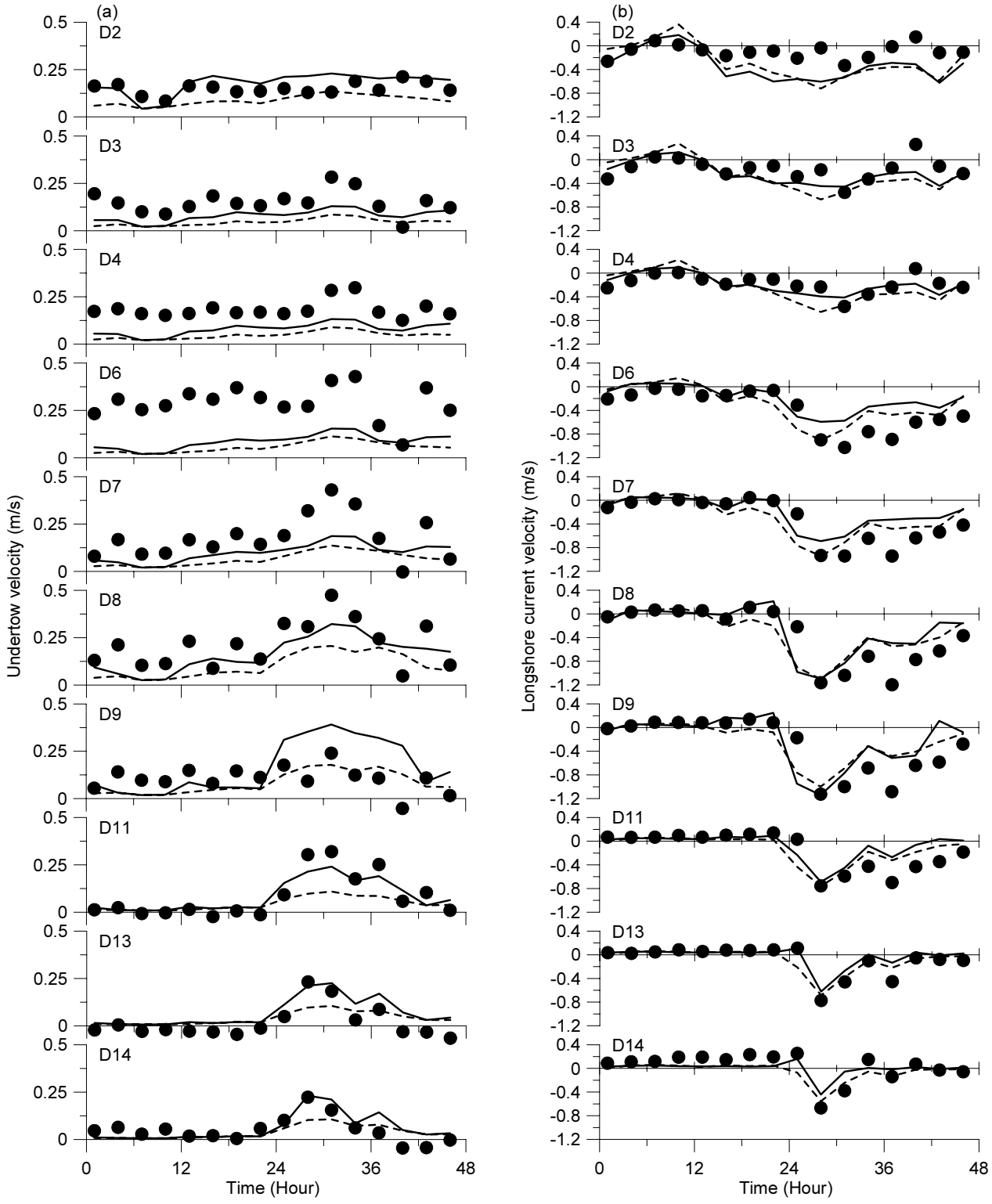

Figure 9 Time series of the undertow (a) and longshore current (b) velocities at Duck. See **Figure 7** for an explanation of graphical symbols.

parametric model tended to underestimate the velocities (**Figures 7, 9, 10, 12 and 13**). The comparisons between the maximum values of the predicted undertow velocities in the bar-trough regions where the cross-shore distances were from 200 m to 350 m at Hasaki and from 180 m to 500 m at Duck and those of the measured values also show that the previous parametric model underestimated the undertow velocity on and around the bar crests (**Figure 14**). Although the present parametric model also mostly underpredicted the undertow velocities near the bar crest at Duck, the predicted values were closer to the measured values than those by the previous parametric model. The assumption of triangular distribution of the cross-shore current velocity in a surface roller with B_r = 0.096 may be better than the assumption of uniform distribution with B_r' = sin(0.05) for the prediction of the undertow velocity near a bar crest.

However, neither the present parametric model nor the previous parametric model was able to reproduce relativelylarge undertow velocities in the trough regions (**Figures 7, 9, 10, 12 and 13**). The velocities predicted by both models rapidly decreased towards the shore after reaching the maximum values near the bar crests, whereas the decreases in the measured values were rather gradual compared to the predicted ones and the measured values remained relatively large even in the trough regions (**Figures 10, 12 and 13**).

Moreover, the present and previous parametric models overestimated the longshore current velocities near the shoreline at Duck (**Figures 9, 10 and 11**). Although the measured values gradually decreased towards the shore near the shoreline, the values predicted by the present and previous parametric models increased again near the shoreline owing to the relatively large wave energy dissipation (**Figures 10 and 11**).

These two discrepancies between the models and the measurements in undertow and longshore current velocities may indicate the limitations of the relatively simple one-dimensional models. In order to increase the accuracy in predicting undertow and longshore current velocities, not only further improvements of the assumptions used in this study such as those for the vertical velocity distribution in a surface roller, the roller dissipation rate and the bottom friction coefficient but also a new approach for modeling hydrodynamics in the nearshore zone may be required.

Probabilistic models are expected to predict sand transport rates more accurately than parametric models because the sand transport rate is strongly influenced by high waves and probabilistic models can predict the transformations of high waves better than parametric models (van Rijn and Wijnberg, 1996). Grasmijer and Ruessink (2003) investigated the difference between the prediction accuracies of parametric and probabilistic models for the undertow and longshore current velocities and obtained the result that the difference is small. Here, the probabilistic model proposed by Kuriyama and Nakatsukasa (2000), which was the basis of the present parametric model as mentioned in Section 2, was chosen and its prediction accuracy was compared with that for the present parametric model.

In the present probabilistic model, the assumption of the roller area being proportional to the square of the wave height used in Kuriyama and Nakatsukasa (2000), as mentioned in Section 2, was replaced by the assumption that the roller evolution is computed by Eq. (9). As the lateral mixing term, Eq. (14) was used instead of that proposed by Battjes (1975) in Kuriyama and Nakatsukasa (2000).

The three free parameters of $B_{r,2}$, ν_2 and $k_{a,2}$, where the suffix 2 indicates the values for the present probabilistic model, were determined in the same way as for the present parametric model, and the best-fit values were $B_{r,2}$ = 0.048, ν_2 = 0.5 m^2/s and $k_{a,2}$ = 0.06 m. The value of $\overline{\varepsilon_{rma,all}}$ was 0.374, which is close to the value of 0.369 for the present parametric model. The relative errors ε_{rma} at measurement locations for the present probabilistic model were also comparable to those for the present parametric model for the undertow and longshore current velocities at Hasaki and Duck (**Figures 15 and 16**). This result is consistent with that in Grasmijer and Ruessink (2003).

7. Conclusions

A one-dimensional parametric model for undertow and longshore current velocities was developed on the basis of the probabilistic model of Kuriyama and Nakatsukasa (2000), which employed the assumption of a triangular velocity distribution in a surface roller and was shown to have good agreements with field data on barred beaches.

The model was compared with field data obtained on barred beaches at Hasaki in Japan and at Duck in the USA as well as two other models, one of which was parametric and

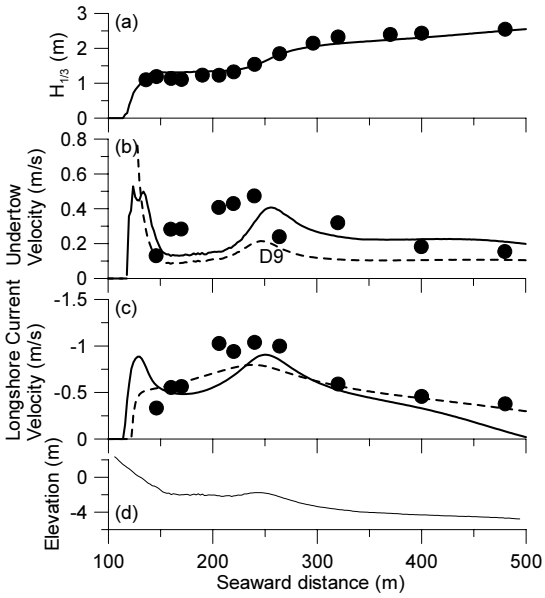

Figure 10 The cross-shore variations of the significant wave height (a), the undertow (b) and longshore current (c) velocities and the elevation (d) at Duck at t = 31 hours. The solid circles show the measured values. The thick solid and broken lines show the vertically averaged values predicted by the present previous parametric models, respectively. Because differences between the vertically averaged values and those at the measurement points in longshore current velocity prediction are small, the latter values are not shown in the figure.

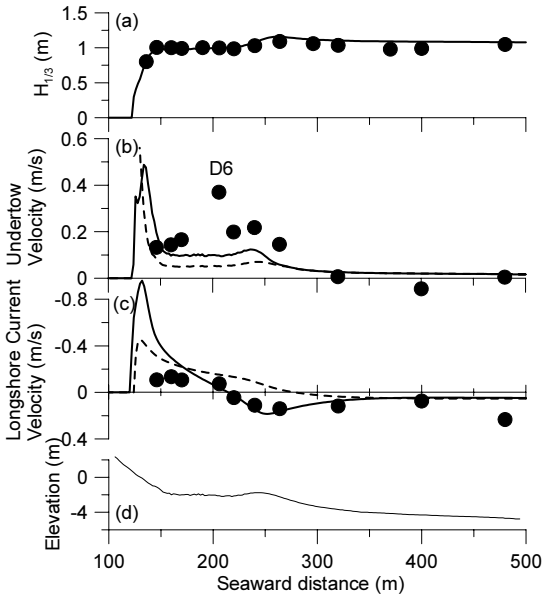

Figure 11 The cross-shore variations of the significant wave height (a), the undertow (b) and longshore current (c) velocities and the elevation (d) at Duck at t = 19 hours. See **Figure 10** for an explanation of graphical symbols.

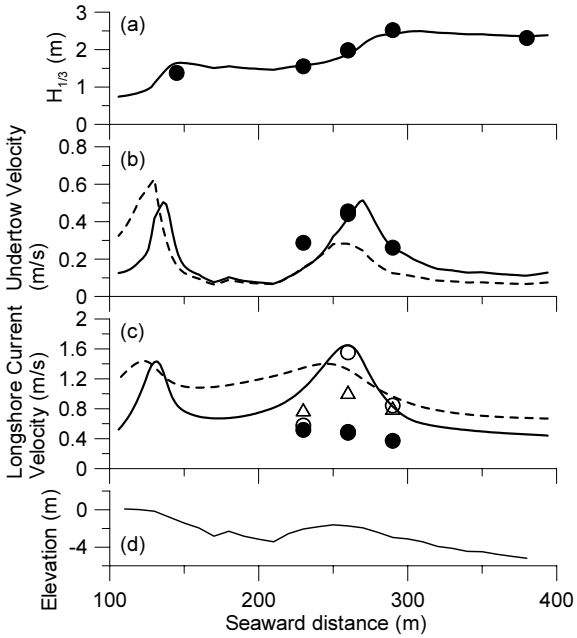

Figure 12 The cross-shore variations of the significant wave height (a), the undertow (b) and longshore current (c) velocities and the elevation (d) at Hasaki at t = 29.5 hours. Open circles and triangles show longshore current velocities predicted at the measurement points by the present and previous parametric models, respectively. See **Figure 10** for an explanation of other graphical symbols.

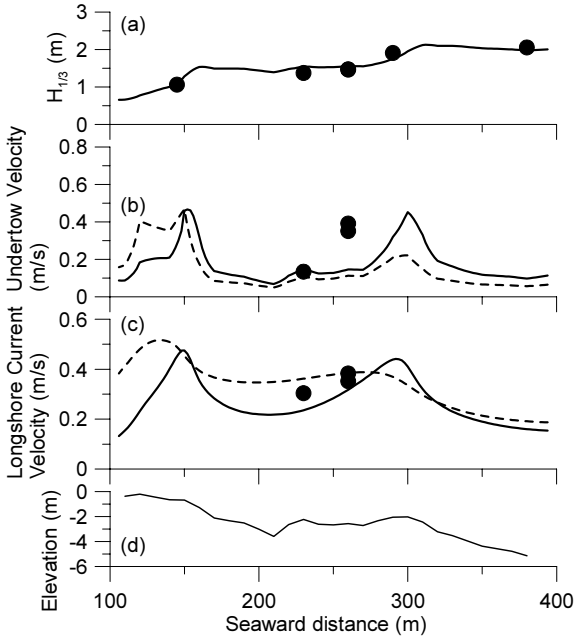

Figure 13 The cross-shore variations of the significant wave height (a), the undertow (b) and longshore current (c) velocities and the elevation (d) at Hasaki at t = 65.5 hours. See **Figure 10** for an explanation of graphical symbols.

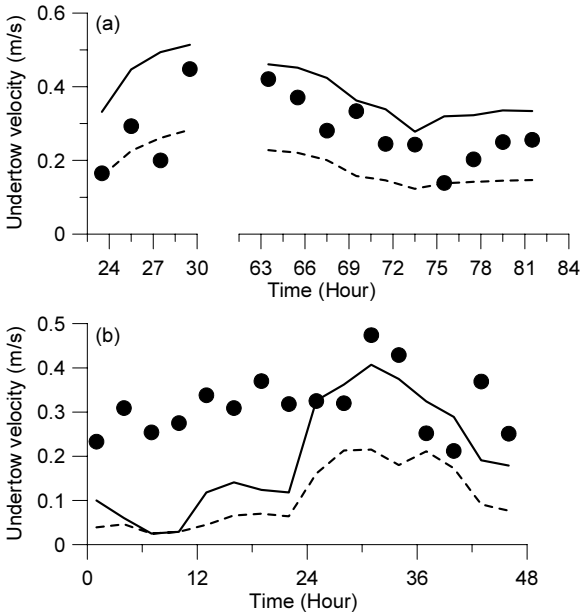

Figure 14 Time series of the maximum undertow velocities in the bar-trough regions at Hasaki (a) and Duck (b). See **Figure 10** for an explanation of graphical symbols.

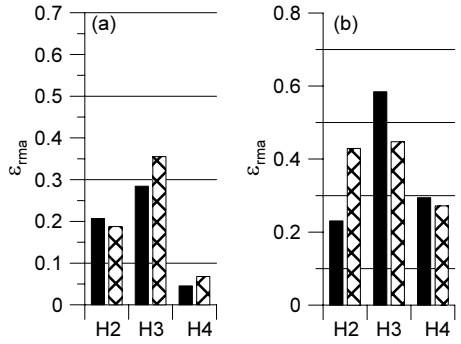

Figure 15 Model error statistics for the undertow (a) and longshore current (b) velocities at Hasaki. The solid and cross-hatched columns show the values for the present parametric and probabilistic models, respectively.

employs the assumption of a uniform velocity distribution in a roller as in Svendsen (1984) and the roller energy dissipation model proposed by Stive and de Vriend (1994) and the other was a probabilistic model based on Kuriyama and Nakatsukasa (2000).

The comparisons showed that the present parametric model predicted the velocity fields at the two sites reasonably well and the prediction accuracy of the present parametric model is slightly better than that of the other two models. The performance of the present parametric model for the undertow

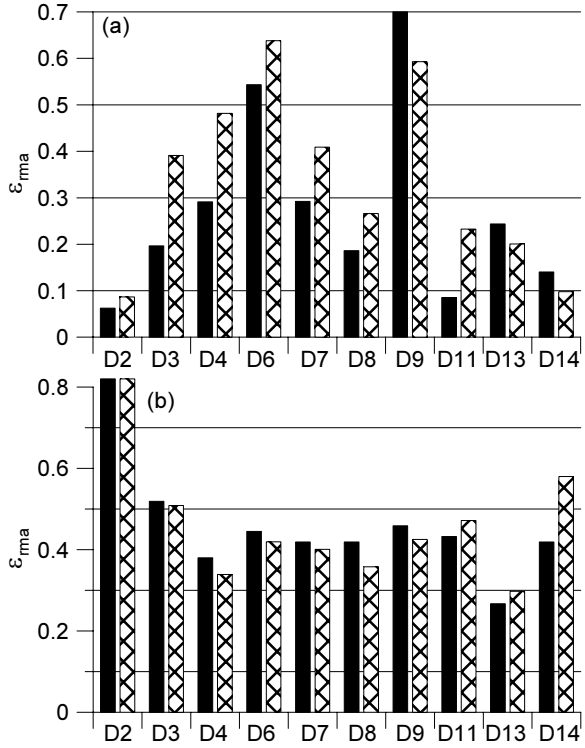

Figure 16 Model error statistics for the undertow (a) and longshore current (b) velocities at Duck. Although ε_{rma} in the longshore current velocity at D2 were 1.66 and 1.29 for the present parametric and probabilistic models, respectively, those values were shown to be 0.82, which is slightly larger than the maximum value on the vertical scale in the figure. See **Figure 15** for an explanation of graphical symbols.

velocity at a single measurement location belonged to the "excellent" category, where the relative mean absolute error ε_{rms} is lower than 0.1 (van Rijn, 2003), at three locations out of 13 at the two sites, to the "good" category ($0.1<\varepsilon_{rms}<0.3$) at eight locations, while that for the longshore current velocity was "good" at three locations and "reasonable" ($0.3< \varepsilon_{rms} <0.5$) at seven locations.

Although the overall prediction of the present parametric model was reasonably good, it underpredicted the undertow velocities in the trough regions. The predicted velocities rapidly decreased towards the shore after reaching the maximum values near the bar crests, whereas the decreases in the measured values were rather gradual. Moreover, the measured values remained relatively large values even in the trough regions. As for the longshore current, the present parametric model overestimated the velocities near the shoreline. Although the measured values decreased gradually

towards the shore near the shoreline, the values predicted by the present parametric model increased again near the shoreline owing to the relatively large wave energy dissipation.

(*Received on January 20, 2010*)

Acknowledgements

Field data obtained at Duck were provided by R.T. Guza and Steve Elgar, who were supported by the US Office of Naval Research, and by the U.S. Army Corps of Engineers', Coastal & Hydraulics Laboratory's, Field Research Facility. The offshore data at Hasaki were provided by Kashima Port Construction Office of Ministry of Land, Infrastructure, Transport and Tourism, and Marine Information Division of Port and Airport Research Institute. The author would like to thank three anonymous reviewers for their useful and thought-provoking comments. All the staff members of HORS are gratefully acknowledged for their contributions to the field measurements.

References

Battjes, J.A. (1975): Modeling of turbulence in the surf zone, *Symposium on Modeling Techniques*, ASCE, pp.1050-1061.

Church, J.C. and Thornton, E.B. (1993): Effects of breaking wave induced turbulence within a longshore current model, *Coastal Engineering,* Vol.20, pp.1-28.

Cox, D.T. and Kobayashi, N. (1998): Application of an undertow model to irregular waves on plane and barred beaches, *Journal of Coastal Research,* Vol.14, No.4, pp.1314-1324.

Dally, W.R. and Brown, C.A. (1995): A modeling investigation of the breaking wave roller with application to cross-shore currents, *Journal of Geophysical Research,* Vol.100, No.C12, pp.24873-24883.

Dally, W.R. and Dean, R.G. (1984): Suspended sediment transport and beach profile evolution, *Journal of Waterway, Port, Coastal and Ocean Engineering,* Vol.110, No.1, pp.15-33.

de Vriend, H.J. and Stive, M.J.F. (1987): Quasi-3D modelling of nearshore currents, *Coastal Engineering* 11, 565-601.

Deigaard, R., Justesen, P. and Fresoe J. (1991): Modelling of undertow by a one-equation turbulence model, *Coastal Engineering,* Vol.15, pp.431-458.

Elgar, S., Guza, R.T., Raubenheimer, B., Herbers, T.H.C. and Gallagher, E.L. (199): Spectral evolution of shoaling and breaking waves on a barred beach, *Journal of Geophysical Research,* Vol.102, No.C7, pp.15797-15805.

Feddersen, F., Guza, R.T., Elgar, S. and Herbers, T.H.C. (1998): Alongshore momentum balances in the nearshore, *Journal of Geophysical Research,* Vol.103, No.C8, pp.15667-15676.

Gallagher, E.L., Elgar, S. and Guza, R.T. (1998): Observations of sand bar evolution on a natural beach, *Journal of Geophysical Research,* Vol.103, No.C2, pp.3203-3215.

Garcez-Faria, A.F., Thornton, E.B., Stanton, T.P., Soares, C.V. and Lippmann, T.C. (1998): Vertical profiles of longshore currents and related bed shear stress and bottom roughness, *Journal of Geophysical Research,* Vol.103, No.C2, pp.3217-3232.

Goda, Y. (1970): A synthesis of breaker indices, *Transactions of Japan Society of Civil Engineers,* Vol.2, No.2, JSCE, pp.227-230.

Goda, Y. (1983): A unified nonlinearity parameter of water waves, *Report of the Port and Harbour Research Institute,* Vol.22, No.3, pp.3-30.

Grasmeijer, B.T. and Ruessink, B.G. (2003): Modeling of waves and currents in the nearshore parametric vs. probabilistic approach, *Coastal Engineering,* Vol.49, pp.185-207.

Haines, J.W. and Sallenger, Jr., A.H. (1994): Vertical structure of mean cross-shore currents across a barred surf zone, *Journal of Geophysical Research,* Vol.99, No.C7, pp.14223-14242.

Kuriyama, Y. (1994): Numerical model for longshore current distribution on a bar-trough beach, *Proceedings of the 24th International Conference on Coastal Engineering*, ASCE, pp.2237-2251.

Kuriyama, Y. (1996): Models of wave height and fraction of breaking waves on a barred beach, *Proceedings of the 25th International Conference on Coastal Engineering*, ASCE, pp.247-260.

Kuriyama, Y. (1998): Field measurements of undertow on longshore bars, *Proceedings of the 26th International Conference on Coastal Engineering*, ASCE, pp.297-310.

Kuriyama, Y. and Nakatsukasa, T. (2000): A one-dimensional model for undertow and longshore current on a barred beach, *Coastal Engineering,* Vol.40, pp.39-58.

Kuriyama, Y. and Ozaki, Y. (1993): Longshore current

distribution on a bar-trough beach –Field measurements at HORF and numerical model-, *Report of the Port and Harbour Research Institute,* Vol.32, No.3, pp.3-37.

Kuriyama, Y. and Ozaki, Y. (1996): Wave height and fraction of breaking waves on a bar-trough beach-Field measurements at HORS and modeling-, *Report of the Port and Harbour Research Institute,* Vol.35, No.1, pp.1-38.

Kuriyama, Y., Ito, Y. and Yanagishima, S. (2008): Cross-shore variation of long-term average longshore current velocity in the nearshore zone, *Continental Shelf Research,* Vol.28, No.3, pp.491-502, doi:10.1016/j.csr.2007.10.008.

Larson, M. and Kraus, N.C. (1991): Numerical model of longshore current for bar and trough beaches, *Journal of Waterway, Port, Coastal, and Ocean Engineering,* Vol.117, pp.326-347.

Lippmann, T.C., Thornton, E.B. and Reniers, A.J.H.M. (1995): Wave stress and longshore current on barred profiles, *Coastal Dynamics '95*, ASCE, pp.401-412.

Longuet-Higgins, M.S. (1970a): Longshore currents generated by obliquely incident waves, 1, *Journal of Geophysical Research,* Vol.75, pp.6778-6789.

Longuet-Higgins, M.S. (1970b): Longshore currents generated by obliquely incident waves, 2, *Journal of Geophysical Research,* Vol.75, pp.6790-6801.

Masselink, G. and Black, K.P. (1995): Magnitude and cross-shore distribution of bed return flow measured on natural beaches, *Coastal Engineering,* Vol.25, pp.165-190.

Nadaoka, K. and Kondoh, T. (1982): Laboratory measurements of velocity filed structure in the surf zone by LDV, *Coastal Engineering in Japan,* Vol.25, pp.125-145.

Nairn, R.B., Roelvink, J.A. and Southgate, H.N. (1990): Transition zone width and implications for modeling surfzone hydrodynamics, *Proceedings of the 22nd International Conference on Coastal Engineering*, ASCE, pp.68-81.

Nishimura, H. (1988): Computation of nearshore current, In: Horikawa, K. (Ed.), *Nearshore Dynamics and Coastal Process –Theory, Measurements and Predictive Models-*. University of Tokyo Press, Tokyo, Japan, pp.271-291.

Okayasu, A., Shibayama, T. and Mimura, N. (1986): Velocity field under plunging waves, *Proceedings of the 20th International Conference on Coastal Engineering*, ASCE, pp.660-674.

Okayasu, A., Shibayama, T. and Horikawa, K. (1988): Vertical variation of undertow in the surf zone, *Proceedings of the 21st International Conference on Coastal Engineering*, ASCE, pp.478-491.

Okayasu, A., Watanabe, A. and Isobe, M. (1990): Modeling of energy transfer and undertow in the surf zone, *Proceedings of the 22nd International Conference on Coastal Engineering*, ASCE, pp.123-135.

Osiecki, D.A. and Dally, W.R. (1996): The influence of rollers on longshore currents, *Proceedings of the 25th International Conference on Coastal Engineering*, ASCE, pp.3419-3430.

Reniers, A.J.H.M. and Battjes, J.A. (1997): A laboratory study of longshore currents over barred and non-barred beaches, *Coastal Engineering,* Vol.30, pp.1-22.

Ruessink B.G., Miles, J.R., Feddersen, F., Guza, R.T. and Elgar, S. (2001): Modeling the alongshore current on barred beaches, *Journal of Geophysical Research,* Vol.106, No.C10, pp.22451-22463.

Seyama, A. and Kimura, A. (1988): The measured properties of irregular wave breaking and wave height change after breaking on the slope, *Proceedings of the 21st International Conference on Coastal Engineering*, ASCE, pp.419-432.

Smith, J.M., Larson, M. and Kraus, N.C. (1993): Longshore current on a barred beach: Field measurements and calculation, *Journal of Geophysical Research,* Vol.98, No.C12, pp.22717-22731.

Smith, J.M., Svendsen, I.A. and Putrevu, U. (1992): Vertical structure of the nearshore current at DELILAH: measured and modeled, *Proceedings of the 23rd International Conference on Coastal Engineering*, ASCE, pp.2825-2838.

Stive, M.J.F., de Vriend, H.J. (1994): Shear stresses and mean flow in shoaling and breaking waves. *Proceedings of the 24th International Conference on Coastal Engineering*, ASCE, pp.594-607.

Stive, M.J.F. and Wind, H.G., 1986. Cross-shore mean flow in the surf zone, *Coastal Engineering,* Vol.10, pp.325-340.

Svendsen, I.A. (1984): Mass flux and undertow in a surf zone, *Coastal Engineering,* Vol.8, pp.347-365.

Thornton, E.B. and Guza, R.T. (1983): Transformation of wave height distribution, *Journal of Geophysical Research,* Vol.88, No.C10, pp.5925-5938.

Thornton, E.B. and Guza, R.T. (1986): Surf zone longshore currents and random waves: field data and models, *Journal of Physical Oceanography,* Vol.16, pp.1165-1178.

van Rijn, L.C., Walstra, D.J.R., Grasmeijer, B., Sutherland, J.,

Pan, S. and Sierra, J.P. (2003): The predictability of cross-shore bed evolution of sandy beaches at the time scale of storms and seasons using process-based profile models, *Coastal Engineering,* Vol.47, pp.295-327.

van Rijn, L.C. and Wijnberg, K.M. (1996): One-dimensional modeling of individual waves and wave-induced longshore currents in the surf zone, *Coastal Engineering,* Vol.28, pp.121-145.

港湾空港技術研究所報告　第 49 巻第 2 号

２０１０．６

編集兼発行人　独立行政法人港湾空港技術研究所

発　行　所　独立行政法人港湾空港技術研究所
横須賀市長瀬３丁目１番１号
TEL. 046(844)5040 URL. http://www.pari.go.jp/

印　刷　所　株式会社　大　應

CONTENTS